JOURNAL OF CATALYSIS 135, 548–562 (1992)

Potassium Promotion of Iron Oxide Dehydrogenation Catalysts Supported on Magnesium Oxide

2. 1-Butene Dehydrogenation Activity

D. E. STOBBE,* F. R. VAN BUREN,* A. J. VAN DILLEN,† AND J. W. GEUS†

*Dow Benelux N.V., P.O. Box 48, 4530 AA Terneuzen, The Netherlands; and †Department of Inorganic Chemistry, State University of Utrecht, P.O. Box 80083, 3508 TB Utrecht, The Netherlands

Received October 3, 1990; revised September 13, 1991

Potassium promotion of iron oxide catalysts supported on magnesium oxide results in considerably more active and selective 1-butene dehydrogenation catalysts. Upon promotion the activation energy was found to decrease from 194 to 156 kJ/mol. $KFeO_2$ appeared to be the active phase under dehydrogenation conditions. No reduction of $KFeO_2$ was observed. $KFeO_2$ shows high 1-butene dehydrogenation activity, yet it is not sufficiently effective to suppress coking entirely. For that purpose the presence of highly dispersed potassium carbonate at the catalyst surface is a prerequisite. Under identical dehydrogenation conditions, a commercial unsupported catalyst, S-105, which contains the more easily reducible $KFe_{11}O_{17}$, is reduced to Fe_3O_4. Compared with this unsupported S-105 catalyst, the supported catalysts show significantly higher 1,3-butadiene selectivities at comparable conversion levels, which is to be attributed to the different natures of their respective active phases.

INTRODUCTION

Part 1 of this work (*1*) has dealt with the structural aspects of potassium promotion of iron oxide catalysts supported on magnesium oxide. This paper is devoted to the catalytic performance and the phase compositions of the potassium-promoted supported catalysts in the dehydrogenation of 1-butene. The MgO-supported catalyst should have the merit of maintaining the mechanical strength during operation (*2*, *3*).

Unpromoted iron oxide catalysts deactivate due to carbon deposition (*4*), but this is suppressed by the presence of potassium as K_2CO_3 (*5–7*). K_2CO_3 is a good catalyst for gasification of carbon (*8*) because of its ability to wet the carbon surface (*9*). The mechanism of the gasification in the presence of alkali is nevertheless still controversial. One proposed mechanism is that gasification proceeds via alkali metal intercalates (*10*, *11*). Others dispute reduction of the alkali metal ions and attribute the catalytic action to the presence of surface structures containing alkali oxide on the carbon (*12*).

Furthermore, potassium is also reported to have a strong promoting effect on the dehydrogenation reaction itself (*13*). According to Lee (*14*), potassium increases the activity of unsupported iron oxide catalysts by more than an order of magnitude. For a better understanding, we should touch on the mechanism of the dehydrogenation reaction. In the past, relatively few kinetic and mechanistic studies have been devoted to catalytic dehydrogenation over iron oxide catalysts (*15–20*). The studies were mainly concerned with ethylbenzene-to-styrene dehydrogenation. Generally, a Langmuir–Hinselwood mechanism is proposed to be applicable to the dehydrogenation reaction. This implies that a surface reaction, e.g., hydrogen abstraction from the reactant, is the rate-determining step. Accordingly, ad- and desorption of both reactants and products must be relatively fast. As Krause (*21*)

0021-9517/92 $5.00

argues, both so-called latent cationic electron donor and latent anionic electron acceptor sites are present on the iron oxide surface. The hydrocarbon reactant, e.g., butene or ethylbenzene, would be rapidly adsorbed onto the cationic donor site by π-bonding of the unsaturated group (*22*). Next, hydrogen abstraction as the rate-determining step requires electron donation from the electron donor site to the α-H atom on the alkyl chain (*21, 22*). Potassium is considered to promote the reaction by facilitating the electron transfer from the electron donor site to the reactant molecule (*13, 23*). Potassium is also supposed to neutralize the acidic acceptor sites, which are responsible for the formation of side products (*13*). The effect of potassium promotion is demonstrated by a higher dehydrogenation activity associated with a lower activation energy (*19*).

To account for the promoter effect, Lee (*14*) and Lee and Holmes (*23*) tried to correlate the activity of iron oxide, promoted with different alkali metal oxides, to the electronic properties of the promoter atom, such as its first ionization potential. This approach, however, is only appropriate when the potassium promoter is present as alkali metal atoms and not as potassium ions. Vijh (*24*) showed a correlation to exist between the ionicity of various alkali metal oxides, on the one hand, and the activity and selectivity of promoted iron oxides, on the other hand. The active sites were considered to be located at or around points on the catalyst surface where the promoter ions are embedded. Other work, such as that of Mross (*13*) and others (*25–33*) cited in the Introduction to Part 1 (*1*), considers the phases likely to be present.

The present paper deals with the 1-butene to 1,3-butadiene dehydrogenation activity of the potassium-promoted supported iron oxide catalysts. The phase composition of the catalyst before and after dehydrogenation has been studied magnetically (*34–36*).

TABLE 1

1-Butene Dehydrogenation Test Conditions

Isothermal experiments	
Pressure	1 bar
Feed rate	50 ml/min
WHSV	0.35 g 1-butene · g/catalyst/h
Feed	5 vol% 1-butene
	30 vol% water
	65 vol% nitrogen
Water/1-butene	6 mol/mol
Temperature	873 K
Temperature-programmed experiments	
Feed	3.6 vol% 1-butene
	30 vol% water
	66.4 vol% nitrogen
Water/1-butene	8.2 mol/mol
Temperature range	723–898 K

EXPERIMENTAL

Catalyst Preparation

Magnesia-supported iron oxide catalysts promoted with potassium were prepared by either consecutive or simultaneous impregnation of a preshaped magnesium oxide support with an iron complex and potassium carbonate, as fully detailed in Part 1 (*1*) and elsewhere (*37*).

1-Butene Dehydrogenation Activity Testing

The activity for the dehydrogenation of 1-butene was determined using an automated flow apparatus, which has been described elsewhere (*4*). About 1 g of catalyst was packed into a quartz fixed-bed flow reactor with an internal diameter of about 8 mm. Previously, the catalyst pellets were fragmented into particles of sizes between 0.5 and 0.85 mm. The test conditions generally used are shown in Table 1. The activity of the catalysts was determined as a function of the temperature. Catalysts were also tested isothermally at 873 K and at a molar steam/1-butene ratio of 6 to determine the stability of the activity. Temperature-programmed experiments were performed at a slightly higher steam/1-butene of 8.2. This allows for the comparison of the kinetic

parameters derived from the temperature-programmed activity measurements with those obtained with the unpromoted catalysts. Under these conditions deactivation of unpromoted supported iron oxide catalysts due to coking is minimized (*4*).

Under the conditions specified in Table 1, 1-butene is, next to being dehydrogenated to 1,3-butadiene, also rapidly isomerized to *cis*-2-butene and *trans*-2-butene. Since the dehydrogenations of 1- and 2-butenes are comparable (*38*), *cis*-2-butene and *trans*-2-butene are not considered as products, but as reactants next to 1-butene. For reasons given elsewhere (*4*), the following definitions for the conversion, the selectivity to product (*i*), and the yield of product (*i*) are used:

$$\text{Conversion (\%)} = \frac{\Sigma\, n(i) \cdot \text{prod.}(i)}{\Sigma\, n(i) \cdot \text{prod.}(i) + \text{butenes(after)}} \cdot 100\% \quad (1)$$

$$\text{Selectivity } i\,(\%) = \frac{n(i) \cdot \text{prod.}(i)}{\Sigma\, n(i) \cdot \text{prod.}(i)} \cdot 100\% \quad (2)$$

$$\text{Yield } i\,(\%) = \frac{n(i) \cdot \text{prod.}(i)}{\Sigma\, n(i) \cdot \text{prod.}(i) + \text{butenes(after)}} \cdot 100\% \quad (3)$$

Prod.(*i*) refers to the concentration of product *i* expressed in mol/liter; *n*(*i*) refers to the ratio between the number of carbon atoms in product *i* and the number of carbon atoms in butene. The term butenes(after) expresses the total amount of unreacted butenes. The term ($\Sigma\, n(i) \cdot$ prod.(*i*) + butenes (after)) is equal to the concentration of butene in the feed expressed in mol/liter. In these calculations carbon deposited on the catalyst is not considered. Unless specified otherwise, kinetic data are expressed per gram of catalyst.

Catalyst Characterization

The phase compositions of the catalysts before and after dehydrogenation were determined by means of high-field magnetic measurements using a modification of the Weiss extraction technique, as described by Selwood (*35*). The apparatus has been described elsewhere (*36*). In view of the sensitivity of $KFeO_2$ toward moisture and carbon dioxide, which causes decomposition of the mixed oxide (*1*), a reactor that allowed the treatment of a catalyst under 1-butene dehydrogenation conditions, prior to the magnetization measurements without intermediate exposure to air, was constructed. After pretreatment in the 1-butene/steam feed, the reactor was purged with nitrogen at 673 K. Thermomagnetic analyses were performed at a field strength of 0.39 MA/m in helium. The magnetization was measured first at increasing temperature and subsequently at decreasing temperature. Before use helium was purified over activated carbon at liquid nitrogen temperature. The amounts of catalyst used were chosen so as to contain equal amounts of iron for each analysis.

X-ray diffraction measurements were performed in a Philips powder diffractometer mounted on a Philips PW-1140 X-ray generator with Fe$K\alpha_{1,2}$ radiation (λ = 1.93735 Å).

RESULTS AND DISCUSSION

1-Butene Dehydrogenation Activity

Nonoxidative dehydrogenation catalysts are commonly operated at temperatures between 850 and 900 K. To determine the catalytic behavior of the potassium-promoted supported iron oxide catalysts as a function of time, the catalysts are operated under dehydrogenation conditions isothermally at 873 K. Results for consecutively and simultaneously impregnated catalysts do not differ significantly. Since changes in the potassium loading are more easily established using the consecutive method, this paper presents the results measured for the consecutively impregnated catalysts.

Figure 1 shows the 1-butene dehydrogenation activity of a 3.1 wt% Fe/MgO catalyst consecutively promoted with 6 wt% K. The 1-butene conversion and the 1,3-butadiene selectivity have been plotted against

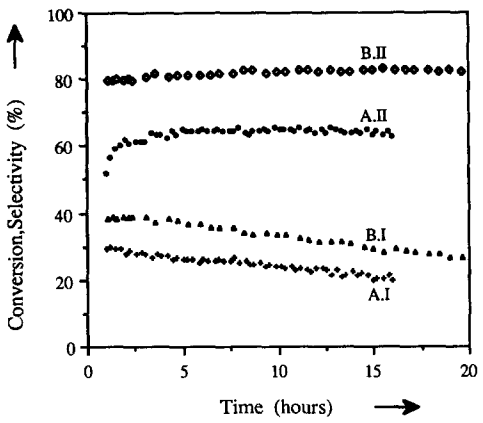

FIG. 1. 1-Butene dehydrogenation activity of a 3.1 wt% Fe/MgO catalyst (A) before and (B) after promotion with 6 wt% K measured isothermally at 873 K at a steam/1-butene ratio of 6 (mol/mol). (I) 1-butene conversion, (II) 1,3-butadiene selectivity.

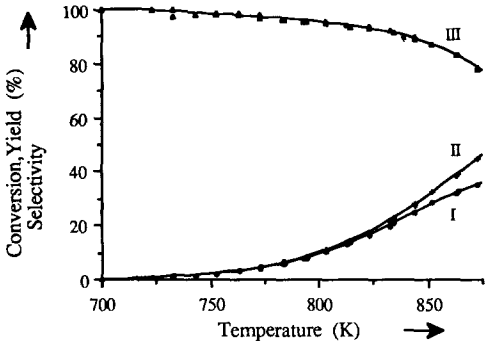

FIG. 2. 1-Butene dehydrogenation activity of a 3.1 wt% Fe/MgO catalyst promoted with 6 wt% K measured as a function of the temperature at a steam/1-butene ratio of 8.2 (mol/mol). (I) 1,3-butadiene yield, (II) 1-butene conversion, (III) 1,3-butadiene selectivity.

time. For comparison the 1-butene dehydrogenation activity of the unpromoted 3.1 wt% Fe/MgO catalyst is also shown. As discussed earlier (*4*), and as shown in Fig. 1, unpromoted magnesia-supported iron oxide catalysts show a strong increase in the 1,3-butadiene selectivity during the first few hours of operation at 873 K. The increase is caused by reduction of the magnesium ferrite phase in the unpromoted catalyst under the influence of the reaction feed. The catalyst is subjected to gradual deactivation due to coking.

As can be seen in Fig. 1, potassium promotion of a 3.1 wt% Fe/MgO catalyst with 6 wt% K results in a substantial increase of both the 1-butene conversion and the 1,3-butadiene selectivity. Neither the iron oxide nor the potassium carbonate separately shows such a high conversion and selectivity. Potassium carbonate supported on MgO is even completely inactive as far as the dehydrogenation of 1-butene is concerned. Remarkably, after promotion with potassium the initial increase in selectivity is absent. Deactivation of the catalyst with time is still present in spite of the presence of 6 wt% K. Although it is not apparent from Fig. 1, deactivation is generally observed to be less severe after promotion with potassium.

The dehydrogenation activity of the 3.1 wt% Fe/MgO catalyst promoted with 6 wt% K has also been determined as a function of temperature at a steam/1-butene ratio of 8.2 mol/mol. The 1-butene conversion, the 1,3-butadiene selectivity, and the 1,3-butadiene yield are shown in Fig. 2. In Fig. 3 the prod-

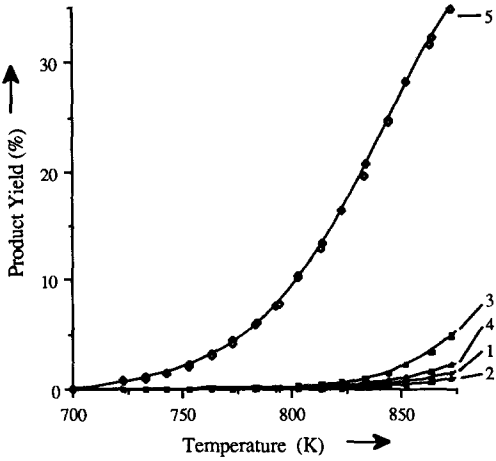

FIG. 3. Product distribution of 1-butene dehydrogenation over a 3.1 wt% Fe/MgO catalyst promoted with 6 wt% K measured as a function of the temperature at a steam/1-butene ratio of 8.2 (mol/mol). (1) methane, (2) ethene, (3) propene, (4) CO_2, (5) 1,3-butadiene.

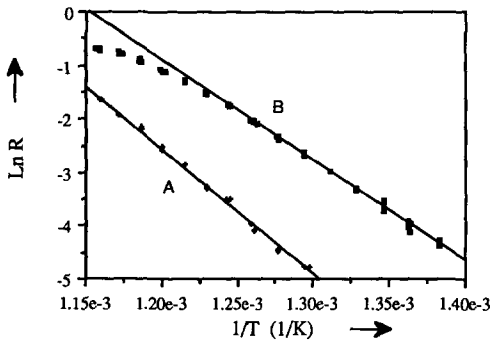

FIG. 4. Arrhenius plot of a 3.1 wt% Fe/MgO catalyst (ex citrate). (A) Unpromoted, (B) promoted with 6 wt% K.

uct distribution is shown. Catalytic dehydrogenation sets in at about 723 K with 100% selectivity. With increasing temperature the 1-butene conversion rises, whereas the 1,3-butadiene selectivity gradually decreases. At 873 K a 1-butene conversion of 45% at a selectivity of 78% is displayed. Accordingly, the 1,3-butadiene yield is 35%, which is far from equilibrium. For comparison, the thermodynamic equilibrium lies at a 62% yield of 1,3-butadiene at 873 K (*39*). At 873 K the main side products are propene and carbon dioxide. In smaller amounts methane and ethene are also formed. The formation of ethane is negligible. Oligomerization products, i.e., products heavier than C_4 (C_5^+), were not observable with our analysis equipment. However, if they were formed, it would only be in negligible amounts (*38*).

The Arrhenius plot shown in Fig. 4 has been constructed from these data. The logarithmic reaction rate, ln R, is plotted against the reciprocal reaction temperature. The reaction rate is defined as $Y \cdot P_{1\text{-butene}} \cdot \tau^{-1}$, in which Y expresses the 1,3-butadiene yield, $P_{1\text{-butene}}$ the partial pressure of 1-butene in the feed, and τ the residence time in the catalyst bed. For comparison, the Arrhenius plot of the unpromoted 3.1 wt% Fe/MgO catalyst is also shown. To establish whether catalyst deactivation occurred, the activity at each temperature has been measured twice. For both catalysts no systematic deactivation was observed between two measurements at the same temperature. In fact, for the promoted catalyst (B) no deactivation was observed between curves obtained by successively increasing and decreasing the temperature. Although not shown here this was not the case for the unpromoted catalyst (A). The most striking difference between the potassium-promoted and the unpromoted catalyst is the much higher dehydrogenation activity of the former. This was already concluded from the isothermal experiments shown in Fig. 1. However, in Fig. 4 the higher activity is even more evident. At low reaction rates, i.e., under differential conditions, both Arrhenius plots are straight. From the slopes, it can be calculated that the activation energy, E_{act}, for the promoted catalyst is lower than that of the unpromoted catalyst. As seen previously (*4*), the activation energy of the unpromoted catalyst is 194 kJ/mol. The same catalyst promoted with 6 wt% K shows an activation energy of 156 kJ/mol. It can thus be concluded that potassium promotion results in a lowering of the activation energy by about 38 kJ/mol. The kinetic data are summarized in Table 2. Additionally, the activation energies and the corresponding preexponential factors of a 3.1 wt% Fe/MgO catalyst promoted with various amounts of potassium are shown. The average activation energy of the potassium promoted catalysts (ex citrate) is 156 kJ/mol. The experi-

TABLE 2

Kinetic Data of Supported Iron Oxide Catalysts

Catalyst	wt% Fe	wt% K	E_{act} (kJ/mol)	ln k_0[a,b]
Fe/MgO	3.1	—	194	25.6
K,Fe/MgO (citrate)	3.1	1.0	157	21.7
K,Fe/MgO (citrate)	3.1	3.0	156	21.7
K,Fe/MgO (citrate)	3.1	6.0	156	21.6
K,Fe/MgO (EDTA)	2.8	3.0	158	21.7
K,Fe/MgO (EDTA)-air[c]	2.8	3.0	155	21.4

[a] [k_0] = atm/min/g cat.
[b] For K,Fe/MgO catalysts, ln k_0 was calculated with E_{act} = 156 kJ/mol.
[c] Exposed to atmospheric air.

mental error in this value is estimated to be about 1 kJ/mol. The activation energy does not depend on the amount of promoting potassium. Remarkably, the logarithmic preexponential factors are also independent of the amount of potassium. Using the value of 156 kJ/mol for the calculation, values of 21.7 are found for the logarithmic preexponential factors. The estimated error in each of the values is about 0.1. The independence of the potassium loading will be explained later on.

At higher rates the Arrhenius curve of the promoted catalyst deflects. This is not caused by diffusion phenomena. The influence of diffusion of 1-butene within the catalyst bodies has been calculated using the Thiele modulus, as described by Satterfield (*40*). For an effective diffusion coefficient of 0.2078 cm^2/s at a temperature of 873 K, the Thiele modulus has been found to be 0.0047. The effectiveness factor is equal to unity for such small values of the Thiele modulus. It can thus be asserted that internal diffusion does not influence the reaction rate. To establish intraparticle diffusion phenomena experimentally, the use of smaller catalyst particles should render a higher apparent dehydrogenation activity. However, no difference in dehydrogenation activity has been observed using catalyst particles between 0.15 and 0.425 mm in diameter, which confirms the conclusions based on the theoretical calculation.

If the deflection of the Arrhenius plot is not related to diffusion phenomena, it should be caused by a gradual lowering of the selectivity at increasing temperatures. As shown in Fig. 3, especially methane, propene, and carbon dioxide are formed at high temperatures at the expense of 1,3-butadiene. Ultimately, the 1,3-butadiene yield will even decrease with temperature due to increasing contribution of nonselective reactions. As an indication, the gas phase conversion of 1-butene at 873 K is about 4% at a 1,3-butadiene selectivity of only about 40%.

Thus far we have seen that potassium promotion of iron oxide catalysts supported on magnesium oxide, which leads to the formation of potassium ferrite (*1*), results in considerably more active and more selective 1-butene dehydrogenation catalysts. It is therefore of great interest to determine the active phase of this catalyst, which is responsible for the increased catalytic activity, under dehydrogenation conditions.

Phase Composition in 1-Butene Dehydrogenation

The phase composition under 1-butene dehydrogenation conditions of a potassium-promoted iron oxide catalyst supported on magnesium oxide has been studied magnetically using a modified Weiss extraction technique (*35, 36*). A study into the phase composition of potassium-promoted iron oxide catalysts requires special provisions to prevent undesired phase transformations. Thus, potassium ferrite has been found to decompose at room temperature in contact with carbon dioxide and water vapor (*1*). Even contact with atmospheric air has appeared to affect the potassium ferrite. This induced the development of a special reactor to allow for the treatment of a catalyst under 1-butene dehydrogenation conditions, prior to the magnetization measurements without intermediate exposure to air.

In a previous study the phase composition under dehydrogenation conditions of an unpromoted supported iron oxide catalyst has been determined (*4*). The magnesium ferrite phase in the unpromoted catalyst was reduced mainly to antiferromagnetic FeO stabilized in the magnesium oxide support. However, at the surface the stabilization of FeO was less strong and consequently the magnesium ferrite reduced only to Fe_3O_4. Evidently, Fe_3O_4 provided the dehydrogenation activity of the unpromoted catalyst. For convenience, the thermomagnetic analysis diagrams of an unpromoted 5.6 wt% Fe/MgO catalyst, which have been discussed previously (*4*), are shown in Figs. 5A and 5B. The Curie temperatures are indicated by the vertical dashed lines. The solid curve indicates the signal of the empty reac-

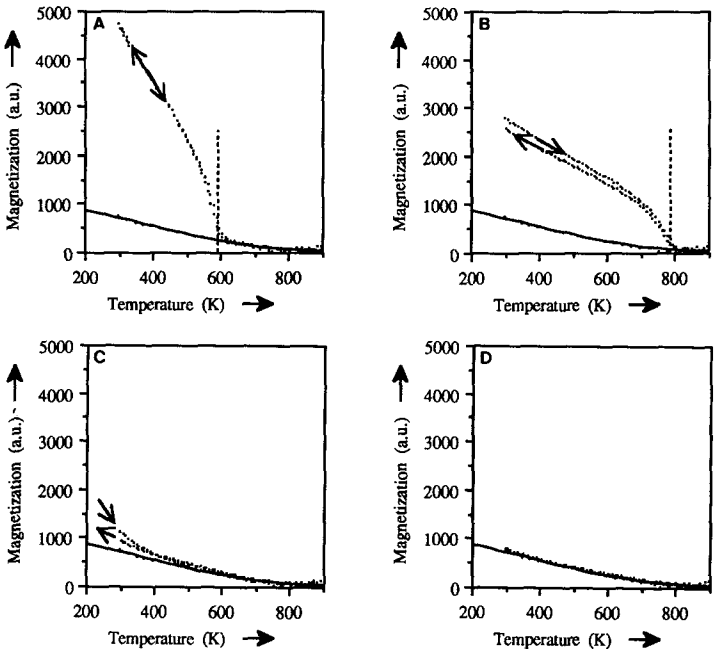

FIG. 5. Thermomagnetic analysis (TMA) diagrams in helium of magnesium oxide supported iron oxide catalysts before and after 4 h use in 1-butene dehydrogenation at 873 K at a steam/1-butene ratio of 6 (mol/mol). The solid curve in the figures indicates the signal of the empty reactor. The vertical dashed line indicates the Curie temperature. (A) 5.6 wt% Fe/MgO catalyst, fresh; (B) 5.6 wt% Fe/MgO catalyst, used; (C) 3.1 wt% Fe/MgO catalyst promoted with 3.0 wt% K, fresh; (D) 3.1 wt% Fe/MgO catalyst promoted with 3.0 wt% K, used.

tor. Figure 5A clearly shows the presence of magnesium ferrite with a Curie temperature at 595 K within the fresh calcined unpromoted catalyst. After dehydrogenation at 873 K, as shown in Fig. 5B, the magnesium ferrite disappeared. The Curie temperature of 790 K is indicative of the presence of Fe_3O_4.

Upon impregnation of a fresh unpromoted supported iron oxide catalyst with potassium carbonate, followed by calcination at 973 K, the magnesium ferrite phase was converted into antiferromagnetic potassium ferrite, $KFeO_2$ (*1*). In the thermomagnetic analysis diagram of the fresh 3.1 wt% Fe/MgO catalyst promoted with 3 wt% K shown in Fig. 5C, the magnetization accordingly decreased to values close to those measured for the empty reactor. The remaining signal of about 400 a.u. originated from a slight amount of unreacted ferrimagnetic magnesium ferrite. Due to the low magnetization, the Curie temperature at 595 K was no longer clearly perceptible. The formation of $KFeO_2$ from $MgFe_2O_4$ upon impregnation with potassium has been discussed previously (*1*).

Next, the promoted catalyst has been subjected to 5 vol% 1-butene and 30 vol% steam in nitrogen at 873 K for 4 h. After this period of time the catalyst was cooled to 673 K and purged with nitrogen. With on-line GC analysis the 1-butene and the water content of the purge gas behind the reactor were monitored. After 1 h all butene and steam had been removed from the gas flow through the reactor. Next, the reactor was cooled to room temperature and transferred to the modified Weiss extraction apparatus. Finally, the thermomagnetic analysis represented in Fig. 5D was performed in helium. By the use of an inert gas, such as helium,

undesired redox phase transformations during the TMA will be prevented at best. After dehydrogenation the magnetization of the promoted catalyst became equal to the signal of the empty reactor. From the absence of Fe_3O_4 and metallic iron, it must be concluded that the potassium ferrite phase was not reduced under the dehydrogenation conditions used here. Reduction of $KFeO_2$ to antiferromagnetic FeO can be excluded, since a stabilizing effect of magnesium oxide on FeO, as has been observed in the unpromoted catalyst, was absent here. Stabilization of FeO would require a practically impossible redissolution of FeO in MgO. The disappearance of the low magnetization of about 400 a.u. observed with the fresh catalyst can be explained by reduction of the remaining magnesium ferrite to antiferromagnetic FeO.

The main conclusion that can be drawn from these experiments is that $KFeO_2$ is not reduced, whereas magnesium ferrite is reduced to FeO and Fe_3O_4 under the dehydrogenation conditions applied here. Evidently, $KFeO_2$ is the active phase in the dehydrogenation of 1-butene to 1,3-butadiene. $KFeO_2$ is thus responsible for the high dehydrogenation activity which is associated with the lowering of the activation energy. The absence of reduction of $KFeO_2$ is also in agreement with the results of temperature-programmed reduction experiments (*1*). In a 10% H_2/Ar flow potassium ferrite appears to be reduced only at much higher temperatures than magnesium ferrite.

When $KFeO_2$ is supposed to be the active phase, the lack of an activation period, as is observed for the 3.1 wt% Fe/MgO catalyst promoted with 6 wt% K in Fig. 1, can be accounted for. The promoted catalyst does not require reduction in order to become active. Consequently, a 3.1 wt% Fe/MgO catalyst promoted with only 1 wt% K should still show an activation period due to reduction of remaining magnesium ferrite. It has been established earlier (*1*) that 1 wt% K is insufficient to convert magnesium ferrite completely into potassium ferrite. Indeed,

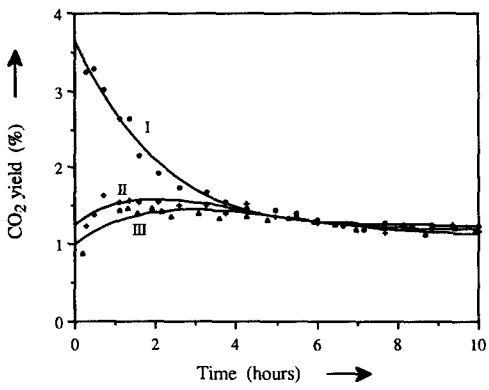

FIG. 6. CO_2 yield of a 3.1 wt% Fe/MgO catalyst promoted with various amounts of potassium during isothermal operation at 873 K at steam/1-butene ratio of 6 (mol/mol). (I) 1 wt% K, (II) 3 wt% K, (III) 6 wt% K.

increases of the 1,3-butadiene selectivity and the yield were observed during the first few hours of isothermal dehydrogenation at 873 K. These increases are due to reduction of the magnesium ferrite by the hydrocarbon feed, which is confirmed by an initially high CO_2 production rate.

In Fig. 6 the CO_2 yield as a function of time is plotted for 3.1 wt% Fe/MgO catalysts promoted with different amounts of potassium ranging between 1 and 6 wt% K. Indeed, the catalyst with only 1 wt% K initially shows a high CO_2 yield of 3.3% due to catalyst reduction, which gradually decreases with time to about 1.1%. The steady yield level of 1.1% CO_2 is not related to catalyst reduction but to CO_2 from gasification under steady operation. The catalyst containing 3 wt% K hardly shows an increased initial CO_2 production, which is indicative of the absence of reduction of the iron species present in the catalyst. With 3 wt% K the conversion of magnesium ferrite into potassium ferrite has been found to be already fairly complete (*1*). The CO_2 production therefore decreases only slightly further upon promotion with a large excess of potassium, i.e., 6 wt% K. The absence of CO_2 production due to catalyst reduction confirms the conclusion drawn from the

TMA results that $KFeO_2$ itself is the active phase in the catalyst under 1-butene dehydrogenation conditions.

Having established that $KFeO_2$ is the active phase, we return to the kinetic data summarized in Table 2. The logarithmic preexponential factors, which are related to the number of active sites, are found to be practically independent of the potassium content in the catalysts. The 3.1 wt% Fe/MgO catalysts promoted with 1 wt% K or 3 wt% K show identical logarithmic preexponential factors of 21.7. Accordingly, the exposed $KFeO_2$ surface area would have to be equal with both catalysts. It can thus be concluded that upon promotion with only 1 wt% K, first the surface of the magnesium ferrite particles is converted to form a surface layer of $KFeO_2$. More potassium carbonate only brings about additional conversion of the bulk of the magnesium ferrite particles into potassium ferrite. The catalyst with 6 wt% K shows a slightly lower logarithmic preexponential factor of 21.6. This would point to the presence of excess potassium carbonate on the potassium ferrite surface and thus some blocking of active sites. However, the difference between the values of 21.6 and 21.7 for the logarithmic preexponential factors is hardly significant.

Influence of Potassium Ferrite Decomposition

Previously, potassium ferrite was found to decompose in atmospheric air at room temperature, due to reaction with carbon dioxide and water vapor to form (hydrated) iron oxide and both potassium carbonate and potassium hydrogen carbonate (*1*). The influence of this decomposition on the activity and stability of the potassium-promoted supported catalysts has also been studied.

In Fig. 7A 1-butene conversion, 1,3-butadiene selectivity, and yield are shown as functions of time for a 4.4 wt% Fe/MgO catalyst promoted with 3 wt% K. The fresh catalyst has been calcined at 973 K followed by cooling to room temperature in dried air. Conversion, selectivity, and yield exhibit the usual behavior. First, reduction of unreacted magnesium ferrite is observed, followed by deactivation due to coking. Evidently, potassium ferrite present in the freshly calcined catalysts is very active and selective in 1-butene dehydrogenation. Although coking is less if compared with the unpromoted supported catalysts, $KFeO_2$ it is not sufficiently effective to suppress coking completely. Obviously, the presence of potassium carbonate at the surface is required. In accordance with this, potassium ferrite is reported to be much less active toward carbon gasification than potassium carbonate (*5–7*). In Fig. 7B the dehydrogenation activity of the same catalyst is shown, but in this case after calcination at 973 K followed by slowly cooling to room temperature in atmospheric air. After this treatment, the presence of $KHCO_3$ has been established using temperature-programmed reduction (*1*). The catalyst now shows a somewhat lower 1-butene conversion at an almost equal 1,3-butadiene selectivity. However, the catalyst does not show deactivation due to coking.

Only after more than 30 h does the catalyst in Fig. 7B start to show slight signs of deactivation. The deactivation can be ascribed to migration of potassium out of the catalyst. The quartz wall of the reactor acts as a sink for potassium. Potassium is known to react extensively with SiO_2 to form potassium silicates (*41*). $K_2Si_2O_5$ and $K_2Si_4O_9$ deposits have been found in the reactor after use, as determined using X-ray diffraction.

Application of an excess of potassium carbonate afterward onto a freshly calcined 3 wt% Fe/3 wt% K/MgO catalyst does not improve the stability. It is very difficult to apply potassium carbonate homogeneously throughout a porous catalyst body by impregnation (*37, 42*); however, it has been established previously using potassium $K\alpha$ linescans that potassium is distributed homogeneously throughout the catalyst pellets (*1*). Evidently, potassium carbonate is required to be distributed homogeneously not only on a macroscopic scale, i.e., through-

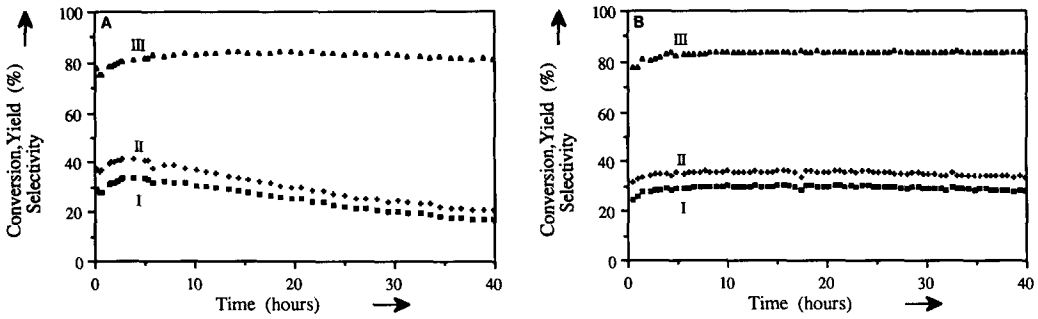

FIG. 7. 1-Butene dehydrogenation activity of a 4.4 wt% Fe/MgO catalyst promoted with 3 wt% K measured isothermally at 873 K at a steam/1-butene ratio of 6 (mol/mol). (I) 1,3-butadiene yield, (II) 1-butene conversion, (III) 1,3-butadiene selectivity. (A) Calcined at 973 K in dried air, (B) calcined at 973 K in atmospheric air.

out the catalyst bodies, but also microscopically, i.e., over the surface of the iron oxide particles, to prevent coking completely. Obviously, a homogeneous distribution over the surface of the iron oxide is accomplished only by decomposition of the potassium ferrite phase, when the potassium comes out of the potassium ferrite lattice homogeneously as potassium carbonate. The same effect of decomposition on stability has been observed for catalysts containing 1.7 and 2.8 wt% Fe/MgO promoted with 3 wt% K.

The activation energy, E_{act}, of the potassium-promoted 2.8 wt% Fe/MgO catalyst after exposure to atmospheric air is 155 kJ/mol, which is equal to the values found for the freshly calcined supported catalysts within experimental error. These kinetic data have been added to Table 2. Supposedly, $KFeO_2$ is still the active phase. However, the logarithmic preexponential factor decreases from 21.7 to 21.4, which is indicative of a decrease of the number of active sites. This is in good agreement with a partial decomposition of the potassium ferrite surface layer.

Comparison with an Unsupported Iron Oxide Catalyst, S-105

A commercial unsupported iron oxide catalyst promoted with potassium, which is generally referred to in the literature, is the Shell catalyst, S-105. This catalyst has a nominal composition of 88.0 wt% Fe_2O_3, 2.5 wt% Cr_2O_3, and 9.5 wt% K_2O (*43*). Before use it has a BET surface area of 2 m^2/g. The average pore radius is about 1500 Å, as determined using mercury intrusion. An X-ray diffraction pattern of the fresh catalyst is shown in Fig. 9A. In the fresh catalyst potassium is mainly present as potassium polyferrite, $KFe_{11}O_{17}$. In the literature this compound is sometimes also referred to as $K_2Fe_{22}O_{34}$, which is its unit cell formula (*44*). Next to this compound, α-Fe_2O_3 and also some $K_2CO_3 \cdot \frac{3}{2}H_2O$ and K_2O are present. The 1-butene dehydrogenation activity of this catalyst as a function of time at 873 K is shown in Fig. 8. Whereas the supported

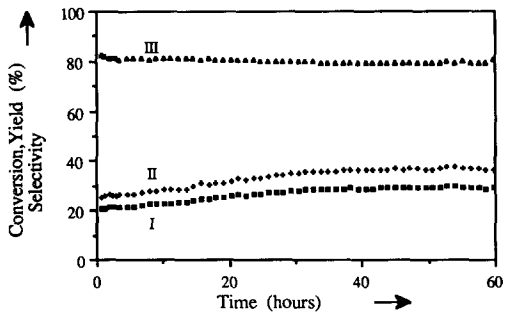

FIG. 8. 1-Butene dehydrogenation activity of the S-105 catalyst as a function of time at 873 K at a steam/1-butene ratio of 6 (mol/mol). (I) 1,3-Butadiene yield, (II) 1-butene conversion, (III) 1,3-butadiene selectivity.

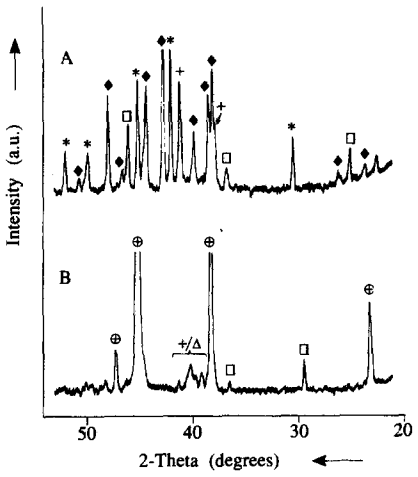

FIG. 9. X-ray diffractograms of the S-105 catalyst. (A) Fresh, (B) after dehydrogenation. (◆) $KFe_{11}O_{17}$, (*) α-Fe_2O_3, (⊕) Fe_3O_4, (+) $K_2CO_3 \cdot \frac{3}{2}H_2O$, (□) K_2O, (△) K_2CO_3.

potassium-promoted catalysts hardly exhibit an activation period, the S-105 catalyst requires about 35 h to reach a steady conversion level of about 36% at a 1,3-butadiene selectivity of 79%. Remarkably, after the initial activation the catalyst does not show signs of deactivation within the first 25 h. The activation period observed here is due to reduction of both α-Fe_2O_3 and $KFe_{11}O_{17}$ to Fe_3O_4 as established using X-ray diffraction after dehydrogenation. The use of Weiss extraction magnetic measurements like those performed on the supported catalysts would not be meaningful, inasmuch as reduction of the antiferrimagnetic $KFe_{11}O_{17}$ (*45*) is obscured by the reduction of α-Fe_2O_3. The X-ray diffraction pattern after dehydrogenation is shown in Fig. 9B. It clearly shows the presence of Fe_3O_4. Potassium is present both as hydrated and as anhydrous potassium carbonate. The activation period being long in comparison with that of the supported catalyst can be explained by the much higher iron oxide content of the unsupported catalyst. It therefore takes longer before all iron oxide has been reduced. Whereas $KFeO_2$ is not reducible under the dehydrogenation conditions used here, evidently, reduction of potassium polyferrites is much more facile and does proceed. According to Courty and Le Page (*27*), the long activation period cannot be fully accounted for by catalyst reduction, but progressive rebuilding of the catalyst surface is also invoked.

After 60 h of isothermal operation at 873 K, the 1-butene dehydrogenation activity of the S-105 catalyst has also been measured as a function of the temperature at a steam/1-butene ratio of 8.2 (mol/mol). From these data the activation energy and the corresponding logarithmic preexponential factor for the unsupported S-105 catalyst are found to be 186 kJ/mol and 26.3, respectively. This activation energy is much higher than the value of 156 kJ/mol observed for the potassium-promoted supported catalyst. It is indicative of the presence of a different active phase, which agrees with the fact that in the unsupported S-105 catalyst α-Fe_2O_3 and $KFe_{11}O_{17}$ are reduced to Fe_3O_4, whereas in the supported catalyst reduction of $KFeO_2$ does not proceed.

The stability of the unsupported catalyst confirms the earlier conclusion that a stable catalyst would require the presence of highly dispersed potassium carbonate at its surface. As we have seen, the $KFe_{11}O_{17}$ phase is reduced to Fe_3O_4 under dehydrogenation conditions. Since Fe_3O_4 does not form a ternary phase with potassium ions (*28*), potassium must come out of the ferrite lattice and then cover the resulting iron oxide homogeneously as potassium oxide, which immediately reacts with the CO_2 produced by catalyst reduction and carbon gasification.

The difference between the performances of the magnesium oxide-supported catalyst and the unsupported S-105 catalyst cannot be derived from the results shown thus far. In order to be able to compare the performances, 1-butene conversions should be compared at equal levels of 1,3-butadiene selectivity. For this purpose the 1,3-butadiene selectivities are plotted against 1-butene conversions in Fig. 10 for both the unsup-

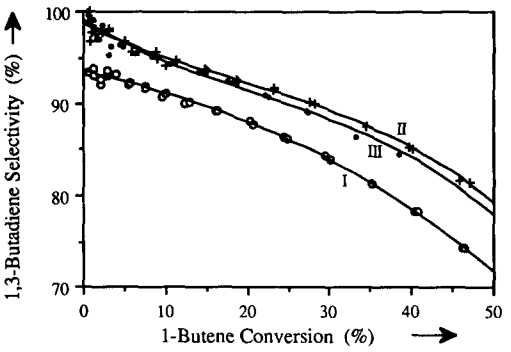

FIG. 10. 1-Butene dehydrogenation performance plot. Data measured at increasing and decreasing temperatures at a steam/1-butene ratio of 8.2 (mol/mol). (I) S-105 catalyst; (II) 2.8 wt% Fe/MgO (EDTA) promoted with 3 wt% K; (III) same as (II), calcined in atmospheric air.

ported S-105 and a 2.8 wt% Fe/MgO catalyst (ex EDTA) consecutively promoted with 3 wt% K. The performance of the supported catalyst after decomposition of $KFeO_2$ in air is shown also. The data have been collected from the 1-butene dehydrogenation activities measured as a function of temperature at a steam/oil ratio of 8.2 (mol/mol). The contact times are equal for all catalysts. Compared with the S-105 catalyst, the freshly calcined supported catalyst shows considerably higher 1,3-butadiene selectivities over the whole range of conversions. The selectivity differences vary from about 4% at low conversion to about 8% at 50% conversion of 1-butene. The curve of the supported catalyst calcined and slowly cooled in atmospheric air runs only slightly below that of the catalyst treated in dried air. This is in accordance with our earlier conclusion that the active phase in both catalysts is the same, i.e., $KFeO_2$.

It is evident that compared with the unsupported S-105 catalyst the supported catalysts show much higher 1,3-butadiene selectivities at comparable 1-butene conversion levels. Figure 10, however, gives no indication about the temperatures required to obtain those conversion levels. For that purpose the temperatures required to reach a 40% 1-butene conversion, which will be referred to as T_{40}, have been collected in Table 3. 1,3-Butadiene selectivities at 40% 1-butene conversion S_{40}, are also given. The potassium-promoted supported catalysts, both prepared from ammonium iron(III) citrate and ammonium iron(III) EDTA, typically require a temperature of 863 to 865 K to obtain 40% conversion of 1-butene. Compared with the supported catalysts, the S-105 catalyst clearly requires a temperature about 8 K higher to reach the same conversion level. However, at the same time the S-105 shows a much poorer selectivity. The supported catalyst calcined in atmospheric air, which appears slightly less active based on the kinetic data displayed in Table 2, accordingly shows a considerably higher T_{40} value. In contrast to what is observed for the S-105 catalyst, this does not result in a much lower 1,3-butadiene selectivity, as has already been shown in Fig. 10. Finally, it seems that supported catalysts prepared from ammonium iron(III) citrate render somewhat lower 1,3-butadiene selectivities, viz., about 2% lower than catalysts prepared from ammonium iron(III) EDTA.

Conclusions

Potassium-promoted magnesia-supported iron oxide catalysts show much higher 1-butene dehydrogenation activities and selectivities than the corresponding unpromoted supported catalysts. The activation energy decreases from 194 to 156 kJ/mol upon promotion with potassium, as

TABLE 3

Comparison of Performance Data

Catalyst	T_{40} (K)[a]	S_{40} (%)[a]
S-105	872	78.6
1 wt% K, 3.1 wt% Fe/MgO (citrate)	863	82.9
6 wt% K, 3.1 wt% Fe/MgO (citrate)	865	82.0
3 wt% K, 2.8 wt% Fe/MgO (EDTA)	864	84.9
3 wt% K, 4.4 wt% Fe/MgO (EDTA)	863	84.9
3 wt% K, 2.8 wt% Fe/MgO (EDTA)–air	876	83.9

[a] For explanation of T_{40} and S_{40}, see text.

was earlier reported by Hirano (*19*). The drop of the activation energy indicates that the rate-determining step is facilitated by the presence of potassium. The active phase in the potassium-promoted supported catalysts was found to be a mixed oxide of iron and potassium, i.e., $KFeO_2$, in agreement with others (*30–32*). The conclusion is based on the absence of catalyst reduction as established using thermomagnetic analysis and using CO_2 monitoring during isothermal 1-butene dehydrogenation at 873 K. These observations are in good agreement with the difficult reduction of $KFeO_2$, as observed with TPR experiments (*1*). Whereas in a 10% H_2/Ar flow reduction of magnesium ferrite already sets in at 600 K, reduction of potassium ferrite does not proceed until 770 K.

On the other hand, reduction is observed for the unsupported S-105 catalyst. When fresh, this catalyst contains $KFe_{11}O_{17}$ next to α-Fe_2O_3. Both $KFe_{11}O_{17}$ and α-Fe_2O_3 were found to be reduced to Fe_3O_4 under dehydrogenation conditions. Analogously, Lichtner and Szalek (*46*) reported reduction of $K_2Fe_{12}O_{19}$ under ethylbenzene dehydrogenation conditions. Obviously, potassium monoferrite, i.e., $KFeO_2$, is much more difficult to reduce than potassium polyferrites, as concluded by others (*31, 33, 47, 48*). Molchanov *et al.* (*31*) reported that the reduction of $KFeO_2$ depended strongly on the steam/1-butene ratio. At high steam/1-butene ratios reduction did not proceed. However, at low steam/1-butene ratios $KFeO_2$ was found to be reduced to Fe_3O_4. This reduction led to a decrease of the dehydrogenation activity, which indicates that the activity was due to $KFeO_2$.

The unsupported S-105 catalyst (activation energy of 186 kJ/mol) presents a type of active phase different than that of the promoted magnesia-supported catalyst (activation energy 156 kJ/mol). The value of 186 kJ/mol that we found for 1-butene dehydrogenation is in remarkably good agreement with the values of 180–192 kJ/mol reported by Càrra (*16*), Càrra and Forni (*17*), and Shibata and Kiyoura (*29*) for ethylbenzene-to-styrene dehydrogenation over the same type of unsupported catalyst. Values ranging from 96 to 142 kJ/mol are also reported in the literature (*14, 19, 49, 50*). These values, however, were not obtained under so-called differential conditions, i.e., at relatively low conversion levels and temperatures. It was observed in Figs. 2 and 4 that above 820 K side reactions start influencing the 1,3-butadiene yields, causing a deflection of the Arrhenius plots. Accordingly, lower apparent activation energies will be obtained. Lower activation energies are also expected when the activity is governed by intraparticle diffusion phenomena (*40*). As argued above, this was not the case with the experiments described here. However, it might be an additional explanation for some of the low activation energies reported in the literature.

$KFeO_2$ shows a high activity for the dehydrogenation of 1-butene. Although coking is less than that for the unpromoted supported catalysts, $KFeO_2$ is not sufficiently effective to suppress coking completely. $KFeO_2$ is much less active toward carbon gasification than K_2CO_3 (*5–7*), and the latter appears to be required for effective suppression of carbon deposition. Mere impregnation with an excess of K_2CO_3 does not result in distributions that are sufficiently homogeneous to suppress coking entirely, but this can be accomplished by either partial decomposition of $KFeO_2$ under influence of atmospheric air or reduction of the ternary phase to Fe_3O_4. The latter was only observed for the unsupported S-105 catalyst containing easily reducible $KFe_{11}O_{17}$. In both cases highly dispersed K_2CO_3 is formed on the iron oxide surface, which is capable of preventing carbon accumulation on the iron oxide surface. Previously, it has been established that under the dehydrogenation conditions used here, i.e., at 873 K and a steam/1-butene ratio of 6 (mol/mol), carbon formation is thermodynamically feasible (*4*). Calculations are based on graphite as the stable carbon phase. Accordingly, car-

bon deposition on unpromoted iron oxide catalysts has been established (*4*). Although thermodynamically carbon deposition is also expected in the experiments described in this paper, it is suppressed in the presence of K_2CO_3. The reason is that carbon is assumed to be deposited via highly reactive intermediates, which are rapidly gasified with steam in the presence of K_2CO_3.

The effect of potassium sulfate in the magnesia-supported catalysts, as reported earlier (*1*), remains, as yet, unclear. However, the presence of potassium bound to sulfate is expected not to be beneficial for the stability of the catalytic activity. According to Lee (*14*), binding the potassium in a compound more stable than potassium carbonate lowers its effectiveness as a promoter. The presence of K_2SO_4 might also account for the extensive reaction of the promoter with the quartz reactor wall. In reducing atmospheres K_2SO_4 is reduced to potassium sulfides (*1*), several of which are known (*51*). Most of them have melting points far below 873 K, thus allowing rapid transport of potassium out of the catalyst bodies. For these reasons the presence of sulfate, which originates from the MgO support, seems undesirable.

Comparison of the performance of our MgO-supported catalysts with the unsupported S-105 catalyst shows that the former combines high 1-butene conversions with 1,3-butadiene selectivities considerably higher than those of the latter. The difference in performance cannot be attributed to differences between textures. Selective dehydrogenation requires relatively small catalyst bodies with relatively wide pores and a relatively small surface area in order to establish fast transport of reactants and products (*14*). Small pores are considered to be detrimental to the 1,3-butadiene selectivity (*27*). The S-105 catalyst contains wider pores than the magnesia-supported catalysts (*37*). As the difference in performance cannot be attributed to differences in textures, it should be ascribed to the different natures of their respective active phases.

In summary, we have succeeded in preparing a K-promoted MgO-supported iron oxide catalyst with improved catalytic properties. The catalyst combines high 1-butene conversions with higher 1,3-butadiene selectivities than a commonly used unsupported iron oxide catalyst, such as the S-105 catalyst. After the proper treatment, as has been described, coking is suppressed also. Using a support, it is expected additionally, that, the catalyst will not exhibit a decreasing mechanical stability. Furthermore, we have been able to establish the effect of potassium promotion and clarify the nature of the active phase.

REFERENCES

1. Stobbe, D. E., van Buren, F. R., van Dillen, A. J., and Geus, J. W., *J. Catal.* **135,** 533 (1992).
2. Stobbe, D. E., Ph.D. thesis, Utrecht (1990).
3. Stobbe, D. E., van Buren, F. R., Groenendijk, P. E., van Dillen, A. J., and Geus, J. W., *J. Mater. Chem.* **1**(4), 539 (1991).
4. Stobbe, D. E., van Buren, F. R., Hoogenraad, M. S., van Dillen, A. J., and Geus, J. W., *J. Chem. Soc. Faraday Trans.* **87**(10), 1639 (1991).
5. Babenko, V. S., Buyanov, R. A., and Afanas'ev, *Kinet. Catal.* **23,** 105 (1982).
6. Babenko, V. S., Buyanov, R. A., and Afanas'ev, A. D., *Kinet. Catal.* **23,** 827 (1982).
7. Babenko, V. S., and Buyanov, R. A., *Kinet. Catal.* **27,** 441 (1986).
8. Hirsch, R. L., Gallagher, J. E., Lessard, R. R., and Wesselhoff, R. D., *Science* **215,** 121 (1982).
9. Mims, C. A., Chludzinski, J. J. Jr., Pabst, J. K., and Baker, R. T. K., *J. Catal.* **88,** 97 (1984).
10. Wen, W.-Y., *Catal. Rev.-Sci. Eng.* **22,** 1 (1980).
11. McKee, D. W., and Chatterji, D., *Carbon* **13,** 381 (1975).
12. Freriks, I. L. C., van Wechem, H. M. H., Stuiver, J. C. M., and Bouwman, R., *Fuel* **60,** 463 (1981).
13. Mross, W. D., *Catal. Rev.-Sci. Eng.* **23,** 591 (1983).
14. Lee, E. H., *Catal. Rev.* **8**(2), 285 (1973).
15. Wenner, R. R., and Dybdal, E. C., *Catal. Eng. Prog.* **45,** 275 (1948).
16. Càrra, S., *Chim. Ind.* **45,** 949 (1963).
17. Càrra, S., and Forni, L., *Ind. Eng. Chem. Process Des. Dev.* **4,** 281 (1965).
18. Andrei, G., Serban, G., and Florita, C., *Rev. Roum. Chim.* **19,** 727 (1974).
19. Hirano, T., *Appl. Catal.* **26,** 65 (1986).
20. Bhat, Y. S., *Indian Chem. Eng.* **30,** 43 (1988).
21. Krause, A., *Sci. Pharm.* **38,** 266 (1970).
22. Busca, G., Zerlia, T., Lorenzelli, V., and Girelli, A., *React. Kinet. Catal. Lett.* **27,** 429 (1985).

23. Lee, E. H., and Holmes, L. H., Jr., *J. Phys. Chem.* **67,** 947 (1963).
24. Vijh, A. K., *J. Chim. Phys.* **72,** 5 (1975).
25. Muhler, M., Schlögl, R., and Ertl, G., *Surf. Interface Anal.* **12,** 233 (1988).
26. Muhler, M., Schlögl, R., and Ertl, G., *in* "Proceedings, 9th International Congress on Catalysis, Calgary, 1988" (M. J. Phillips and M. Ternan, Eds.), Vol. 4, p. 1758. Chem. Institute of Canada, Ottawa, 1988.
27. Courty, P., and Le Page, J. F., *in* "Preparation of Catalysts" (B. Delmon, P. Grange, P. Jacobs, and G. Poncelet, Eds.), Vol. II, Studies in Surface Science and Catalysis, Vol. 3, p. 293. Elsevier, Amsterdam, 1979.
28. Dry, M. E., and Ferreira, L. C., *J. Catal.* **7,** 352 (1967).
29. Shibata, K., and Kiyoura, T., *Bull. Chem. Soc. Jpn.* **42,** 871 (1969).
30. Hirano, T., *Appl. Catal.* **26,** 81 (1986).
31. Molchanov, V. V., Andrushkevich, M. M., Plyasova, L. M., and Kotel'nikov, G. R., *Kinet. Catal.* **29,** 1107 (1988).
32. Muhler, M., Schlögl, R., Reller, A., and Ertl, G., *Catal. Lett.* **2,** 201 (1989).
33. Dejaifve, P. E., Darnanville, J.-P., Garin, R. A. C., Clement, J. C., and Lambert, J. C., EP A- 0,339,704 (1989).
34. Stobbe, D. E., van Buren, F. R., Stobbe-Kreemers, A. W., van Dillen, A. J., and Geus, J. W., *J. Chem. Soc. Faraday Trans.* **87**(10), 1631 (1991).
35. Selwood, P. W., "Chemisorption and Magnetization." Academic Press, New York, 1975.
36. Kock, A. J. H. M., de Bokx, P. K., Boellaard, E., Klop, W., and Geus, J. W., *J. Catal.* **96,** 468 (1985).
37. Stobbe, D. E., van Buren, F. R., Stobbe-Kreemers, A. W., Schokker, J. J., van Dillen, A. J., Geus, J. W., *J. Chem. Soc. Faraday Trans.* **87**(10), 1623 (1991).
38. Kearby, K. K., *Ind. Eng. Chem.* **42,** 295 (1950).
39. Stull, D. R., Westrum, E. F. Jr., and Sinke, G. C., "The Chemical Thermodynamics of Organic Compounds." Wiley, New York, 1969.
40. Satterfield, C. N., "Mass Transfer in Heterogeneous Catalysis." MIT Press, Cambridge, MA, 1970.
41. Perrichon, V., and Durupty, M. C., *Appl. Catal.* **42,** 217 (1988).
42. Neimark, A. V., Kheifez, L. I., and Fenelonov, V. B., *Ind. Eng. Chem. Prod. Res. Dev.* **20,** 449 (1981).
43. Herzog, B. D., and Rase, H. F., *Ind. Eng. Chem. Prod. Res. Dev.* **23,** 187 (1984).
44. Rooymans, C. J. M., Langereis, C., and Schulkes, J. A., *Solid State Commun.* **4,** 85 (1965).
45. Schieber, M. M., *in* "Selected Topics in Solid State Physics" (E. P. Wohlfarth, Ed.), Vol. 8. North-Holland, Amsterdam, 1967.
46. Lichtner, E., and Szalek, G., *Chem. Technol.* **20,** 466 (1968).
47. Andrushkevich, M. M., Kotel'nikov, G. R., Buyanov, R. A., Plyasova, L. M., Villert, M. V., and Abramov, V. K., *Kinet. Catal.* **19,** 283 (1976).
48. Andrushkevich, M. M., Plyasova, L. M., Molchanov, V. V., Buyanov, R. A., Kotel'nikov, G. R., and Abramov, V. K., *Kinet. Catal.* **19,** 332 (1978).
49. Hirano, T., *Bull. Chem. Soc. Jpn.* **59,** 2672 (1986).
50. Matsui, J., Sodesawa, T., and Nozaki, F., *Appl. Catal.* **51,** 203 (1989).
51. Weast, R. C., Ed., "Handbook of Chemistry and Physics," 62nd ed., B-131–B-137. CRC Press, Boca Raton, FL, 1981.